Doping efficiency in *n*-type InP nanowires

Lucas V. Besteiro,[1] Luis Tortajada,[1] J. Souto,[1] L. J. Gallego,[1] James R. Chelikowsky,[2] and M. M. G. Alemany[1,*]

[1]*Departamento de Física de la Materia Condensada, Facultad de Física, Universidad de Santiago de Compostela, E-15782 Santiago de Compostela, Spain*

[2]*Center for Computational Materials, Institute for Computational Engineering and Sciences, Departments of Physics and Chemical Engineering, University of Texas, Austin, Texas 78712, USA*

(Received 2 February 2013; revised manuscript received 4 September 2013; published 20 September 2013)

We examine two factors that could limit the doping of *n*-type III-V semiconductor nanowires, namely, the solubility of the dopants and the possible formation of *DX*-like defect centers. We find that it is preferable to dope zinc-blende nanowires via anion substitution as opposed to cation substitution. The comparison with previous work on *n*-type III-V semiconductor nanocrystals also allows us to determine the role of dimensionality and quantum confinement on doping characteristics of materials. Our work is based on quantum calculations of InP nanowires using real-space pseudopotentials constructed within density functional theory.

DOI: 10.1103/PhysRevB.88.115310 PACS number(s): 61.72.Bb, 61.72.U−, 73.22.−f, 71.15.Mb

I. INTRODUCTION

Semiconductor nanowires (NWs) are of notable interest from both fundamental and technological perspectives.[1] Their reduced dimension offers the possibility of tuning electronic and optical characteristics of their macroscopic counterparts by exploiting the effects of quantum confinement. Also, they can transport electrical carriers efficiently and have been demonstrated as building blocks for working electronic and optoelectronic devices within the nanometer regime. As such, semiconductor NWs are seen as materials that will play a prominent role in the future of the semiconductor industry.

However, the reduced dimension in nanostructures can also introduce deleterious factors in the functionalization of devices via *p*-type and *n*-type doping. For example, it has been shown that in semiconductor nanomaterials the solubility of the impurity atom can be reduced when compared to that of bulk materials.[2–4] Moreover, quantum confinement can cause the appearance of defects that inhibit desired characteristics of the impurity states.[4–6] Here we demonstrate two controlling factors in III-V semiconductor NWs that crystallize in the zinc-blende structure. Specifically, we show for *n*-type doped NWs that the solubility of the dopant, as determined from its formation energy, decreases monotonically with the diameter of the nanomaterial. Also, we show that there are preferential locations of the dopant for the stabilization of *DX* defect centers in the NWs. We find that the formation of such defects inhibits the contribution of the dopants to free carriers that limits technological applications of the NWs; i.e., impurity energy levels can be lowered by more than 1 eV within the fundamental gap.

Our results are based on first-principles calculations of InP NWs. The purpose of studying these NWs is twofold. First, *n*-type InP NWs are among the NWs for which very promising advances have been made from experiment, including the functioning as diodes and field effect transistors when assembled with *p*-type InP NWs.[7,8] With our study we intend to provide information that could be useful for designing devices and applications based on *n*-type InP NWs. Second, from a fundamental point of view, we can establish a comparison with our previous work on *n*-type InP quantum dots (QDs) using the same theoretical approach.[5] With it, we intend to determine how the different dimensionality of quantum confinement (two dimensional in NWs, and three dimensional in QDs) can affect characteristic properties of *n*-type doped semiconductor materials.

II. COMPUTATIONAL DETAILS

We perform the calculations using the PARSEC code,[9] which uses a real-space implementation of pseudopotentials constructed within density functional theory (DFT).[10] Within this implementation, the Kohn-Sham equations are solved self-consistently on a three-dimensional cubic grid. Only one parameter, the grid spacing, controls numerical convergence once the physical domain is set. The core electrons are represented by norm-conserving pseudopotentials.[11] The local density approximation (LDA) is used for the exchange and correlation potential.[12] Besides its accuracy and its inherent efficiency on highly parallel computational platforms, PARSEC offers flexibility in imposing different types of boundary conditions, such as one-dimensional periodic boundary conditions adequate for studying NWs. We have satisfactorily used the PARSEC code in studying several doped InP materials, including the *p*-type bulk,[13] *p*-type NWs,[14] and *p*- and *n*-type QDs.[5,15]

We construct cylindrical models of InP NWs with diameters 0.94, 1.41, and 1.88 nm. The NWs are oriented along the $\hat{z} \equiv [111]$ direction of the zinc-blende structure and passivated with fractionally charged hydrogen-like atoms.[16] We dope NWs to be *n*-type by introducing impurity atoms at both cation and anion sites in the center of the wire. We use a Si atom that substitutionally replaces the cation ($\mathrm{Si_{In}}$), and a Se atom that substitutionally replaces the anion ($\mathrm{Se_P}$). We consider six InP layers along $\hat{z}$ that are replicated in space following one-dimensional periodic boundary conditions; i.e., we consider a one-dimensional supercell two times larger than the primitive cell that includes three InP layers along $\hat{z}$. We do this in order to reduce impurity-impurity interactions (the dopants are separated by $2 \times \sqrt{3}\,a$ along $\hat{z}$, with a being the bulk lattice constant). We sample the one-dimensional Brillouin zone at the Γ point. In the $\hat{x}$ and $\hat{y}$ directions, we chose a cylindrical physical domain with a radius large

 ©2013 American Physical Society

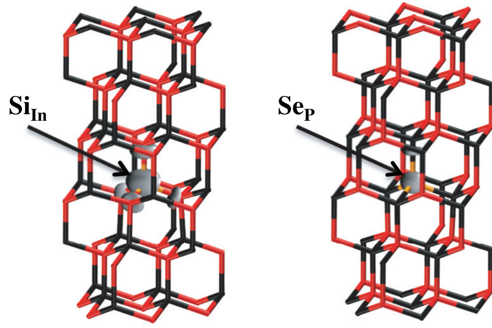

FIG. 1. (Color online) Charge density associated with the donor state introduced in the InP NW with diameter 0.94 nm by Si_{In} (left panel) and Se_P (right panel) n-type doping. Black and red symbols stand for In and P atoms, respectively. Charge density is plotted at 40% of its maximum value.

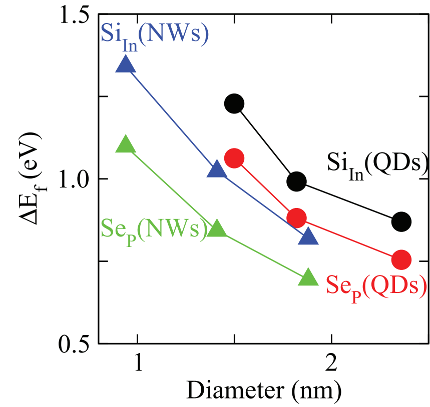

FIG. 2. (Color online) Relative formation energies of Si_{In} and impurities introduced in InP NWs as obtained from first-principles calculations (triangles). The formation energies obtained for the same impurities in a previous study of InP QDs are also shown (circles; Ref. 5). All the results represented were obtained using the same theoretical approach (see the text).

enough to allow the Kohn-Sham wave functions to vanish at its boundary. All the atoms in the NWs were allowed to relax except those at the surface.[4,5] We introduce this constraint in order to replicate experimental conditions: InP NWs are coated with amorphous overlayers.[7,17] The main effect of the overlayers is to passivate chemically the nanomaterials, but they also reduce the role of relaxation of the outermost atoms in the NWs.

III. RESULTS AND DISCUSSION

We are interested in the efficiency of n-type doping by studying the formation energy of the dopants and the possible formation of DX defect centers in the NWs, as we did in our previous work on n-type InP QDs.[5] The formation energy affects doping efficiency as it is a measure of the energy cost derived from the introduction of the dopant into the host material. DX centers are among the most relevant defects that can be present in n-type doped II-VI and III-V semiconductors,[18,19] and could impede the doping of the NWs by inducing a shallow-to-deep transition of the donor states. We perform studies for cation and anion substitution in order to establish preferential doping sites.

n-type doping InP NWs introduces a singly degenerate impurity state with a_1 symmetry and dominant s character, as shown in Fig. 1. The formation energy of the dopant, E_f, can be obtained as

$$E_f(X_Y) = E_{T,\mathrm{NW}}(X_Y) - E_{T,\mathrm{NW}}(\mathrm{undoped}) + \mu(\mathrm{Y}) - \mu(\mathrm{X}), \quad (1)$$

where $E_{T,\mathrm{NW}}$ represent the total energy of the nanomaterial, μ corresponds to the chemical potentials of the elements that are exchanged in the NW, and $X_Y = \{\mathrm{Si_{In}}, \mathrm{Se_P}\}$. The chemical potentials refer to the energy of the particle reservoirs from which the atoms are taken and depend on the working environment. Their appearance in equations can be avoided if one focuses on the effects that quantum confinement has on the formation energy, i.e., by computing the formation energy relative to the bulk,

$$\Delta E_f(X_Y) = [E_{T,\mathrm{NW}}(X_Y) - E_{T,\mathrm{NW}}(\mathrm{undoped})] - [E_{T,\mathrm{bulk}}(X_Y) - E_{T,\mathrm{bulk}}(\mathrm{undoped})], \quad (2)$$

where $E_{T,\mathrm{bulk}}$ represents the total energy of the bulk system.

In Fig. 2, the formation energy for both Si_{In} and Se_P impurities increases monotonically with decreasing diameter of the NWs (triangles). This similar behavior of the formation energies can be explained as result of quantum confinement. In semiconductor nanomaterials, quantum confinement opens the fundamental gap of the bulk materials by increasing and decreasing the conduction band minimum (CBM) and valence band maximum (VBM) energy levels, respectively. The impurity states represented in Fig. 1 possess dominant CBM s character and react similarly to confinement as the CBM state, i.e., impurity energy levels move up with a decreasing diameter of the NW, or increasing quantum confinement. Such an increase in the energy of the single-occupied impurity states reflects in the total energy of the doped nanomaterials giving an increase of the formation energy of the impurities as in Eq. (2). Our study predicts a lower impurity concentration in n-type InP NWs when compared to the bulk because of energetic or thermodynamic arguments. This doping limitation is more relevant for the smaller NWs, and occurs for dopants placed at cation or anion sites. We find quantitative differences that are in favor of the latter.

In Fig. 2 we also represent the formation energies of Si_{In} and Se_P impurities in InP QDs as obtained in our previous study (circles).[5] These data corroborate the increase in formation energies as result of quantum confinement, i.e., as an intrinsic property of nanomaterials. In the nanocrystals, the same electronic structure arguments apply. The electronic states are confined in a three-dimensional physical domain, which reflects in higher formation energies than in the NWs, where the electronic states are confined only in the radial dimension. We predict an increase in the formation energies of the dopants with decreasing dimensionality of the nanomaterials or increasing dimensionality of quantum confinement.

In contrast to the role of formation energies, we determine the location of the impurity to be crucial in forming DX-like defect centers in n-type InP NWs. These centers correspond to negatively charged defects in which either the donor atom or one of its neighbors undergoes a bond-breaking

displacement that introduces a deep level in the band gap and inhibits the electrical activity of other donors.[18,19] In bulk systems, the DX-like defect centers can appear as result of increasing hydrostatic pressure or alloying. Recent theoretical work on semiconductor quantum dots shows that DX centers can also occur as result of the three-dimensional quantum confinement.[4,5]

The highly anisotropic nature of the NWs requires one to differentiate between DX-associated bond breaking along the axial direction and along the radial dimension. The former corresponds to a displacement along $\hat{z} \equiv [111]$, while in the latter the bond is broken along one of the equivalent $[1\bar{1}\bar{1}]$, $[\bar{1}1\bar{1}]$, and $[\bar{1}\bar{1}1]$ zinc-blende crystal directions. Defining a configuration coordinate, Q, as the displacement of the dislocated atom with respect to its ideal or undistorted position allows us to track the energetics associated with the formation of DX-like defect centers in the NWs. The formation energy of a DX center is determined by a direct comparison between the total energy of the negatively charged DX center and the total energy of the negatively charged fourfold-coordinated substitutional donor.[20]

In the upper panel of Fig. 3, we present configuration diagrams obtained for the $\mathrm{Si_{In}}$-doped InP NWs both for axial and radial bond-breaking displacements (circles). We find the negatively charged NWs present three local minimum configurations for all the diameters studied. One of these minima ($Q = 0$) corresponds to $\mathrm{Si_{In}^-}$, in which the extra electron in the NWs is trapped at the impurity donor state as represented in Fig. 1. The other two local minimum configurations ($Q \sim 2.5$ a.u.) correspond to the formation of the DX centers, which result from the displacement of the Si atom along one of the four tetrahedral directions (axial or radial), and adopting an interstitial site (middle panel of Fig. 3).

The transformation from $\mathrm{Si_{In}^-}$ to DX can be understood as driven by electrostatic forces. At $Q = 0$ the negatively charged Si atom is bonded to four anion P atoms so it experiences a repulsive Coulombic force, overcoming the energy barrier that is derived from the breaking of one of the Si-P bonds. In the DX configurations, the negatively charged Si atom is bonded to three P atoms, having as next neighbors three cation In atoms. The electrostatic interactions in the NW are expected to decrease as the diameter increases since the electronic wave functions become more delocalized in space. Energy barriers increase monotonically with increasing diameter, as occurs for axial displacements (0.30 eV, 0.46 eV, and 0.70 eV for the NWs with diameters 0.94 nm, 1.41 nm, and 1.88 nm, respectively). Radial atomic displacements exhibit the same trend, although with some variations that might be attributed to surface effects, i.e., due to the proximity of the dislocated atom to the surface.

The displacement of the impurity Si atom to give DX centers in the NWs significantly lowers the position of the impurity donor state within the energy gap, as is shown in the lower panel of Fig. 3. During displacement, as Q increases, the impurity state couples with an empty state acquiring dominant p character, which is not characteristic of the CBM state. In the case of axial bond breaking, this state is an empty state having a_1 symmetry, a_{1c}. For radial displacements, it is a state having a_1 symmetry that results from the splitting of a doubly degenerate state with e symmetry in the conduction band, $a_1(e_c)$. This splitting is consistent with a reduction of the

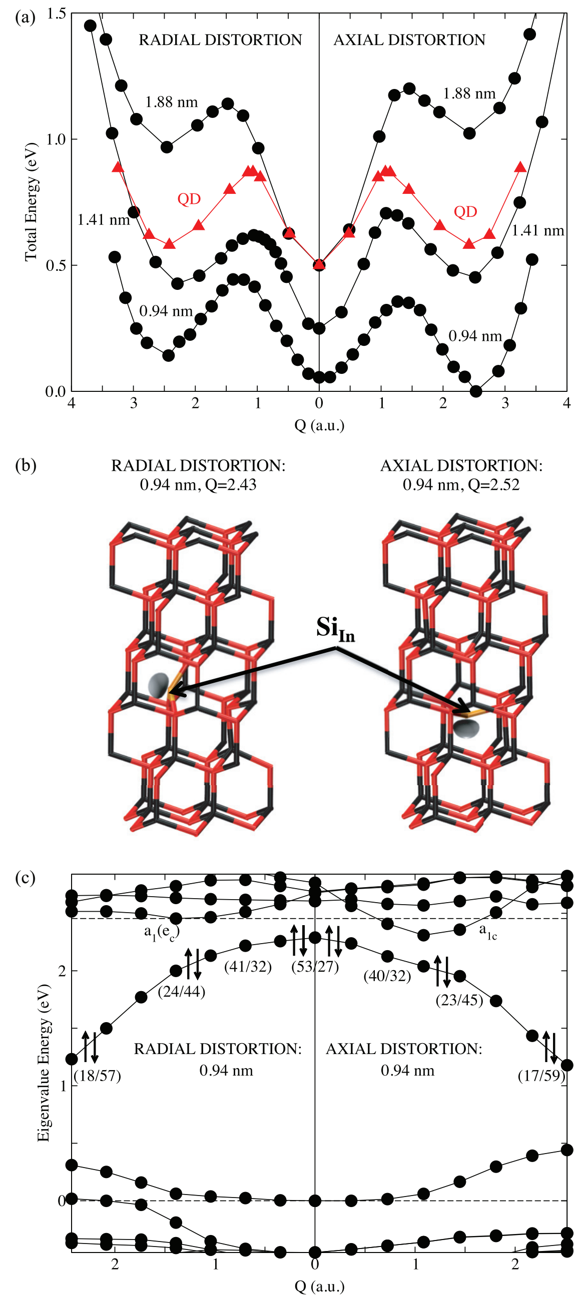

FIG. 3. (Color online) (a) Configuration coordinate diagrams of negatively charged $\mathrm{Si_{In}}$-doped InP NWs obtained for axial and radial atomic displacements (circles). The configuration diagram of the negatively charged $\mathrm{Si_{In}}$-doped InP QD with diameter 1.82 nm obtained in our previous work using the same theoretical approach is also shown (triangles; Ref. 5). (b) DX centers corresponding to the $\mathrm{Si_{In}}$-doped InP NW with diameter 0.94 nm obtained by axial and radial atomic displacements. The charge density associated with the eigenstate holding the donor-electron pair is also shown. Black and red symbols stand for In and P atoms, respectively. Charge density is plotted at 40% of its maximum value. (c) Electronic structure of the negatively charged $\mathrm{Si_{In}}$-doped InP NW with diameter 0.94 nm obtained for axial and radial atomic displacements. The arrows represent the impurity state holding the donor-electron pair, and the numbers in parentheses its projected s/p characters. Dashed lines correspond to CBM and VBM energy levels of the undoped NW that are used as a reference.

ionic symmetry in the NW during atomic displacement. The result is similar in both axial and radial cases; the impurity level becomes a deep state. The electronic energy gain derived from this interaction increases as the diameter of the NW decreases. Since the impurity state in a DX configuration has dominant non-CBM character it does not go up in energy as rapidly as it does at $Q = 0$ due to quantum confinement, so the difference between energy levels at both configurations increases with decreasing diameter of the NW. For axial (radial) atomic displacements such differences are 1.11 eV (1.06 eV), 0.94 eV (0.91 eV), and 0.75 eV (0.74 eV) for the NWs with diameters 0.94 nm, 1.41 nm, and 1.88 nm, respectively.

The electrostatic and electronic structure arguments we present explain the configuration coordinate diagrams for the n-type NWs that are shown in the upper panel of Fig. 3. The DX centers become progressively more relevant as the size of the NWs is reduced, even emerging as the global minimum configuration for the smallest NW with axial atomic displacement. Differences between axial and radial dislocations only appear for the smaller NWs owing to surface effects. Such differences become marginal as the size of the NWs increases.

In the upper panel of Fig. 3 we also represent the configuration diagram obtained for a Si_{In}-doped InP QD (triangles) with diameter similar to that of the biggest NW we studied.[5] In the nanocrystals, the differentiation between axial and radial atomic displacements does not hold. The symmetry of the crystal is preserved, and displacements along the four [111], $[1\bar{1}\bar{1}]$, $[\bar{1}1\bar{1}]$, and $[\bar{1}\bar{1}1]$ zinc-blende crystal directions give the same results (we have extended the configuration coordinate diagram along axial and radial displacements for plotting purposes; the diagram is symmetric with respect to $Q = 0$). The comparison between the two upper curves in Fig. 3(a) clearly shows the effect that the different dimensionality of nanomaterials has on the formation of DX centers; i.e., the formation is favored when the dimensionality is reduced. In the nanocrystals, the wave functions are more localized in space, so the electrostatic interactions become stronger. This explains the lower energy barrier for the Si_{In}^{-} to DX transformation in the depicted QD than in the NW with diameter 1.88 nm (0.37 eV and 0.70 eV, respectively). Also, the higher dimensionality of quantum confinement in the QDs makes the electronic energy gain derived from the lowering of the position of the donor impurity state during the defect formation bigger [0.97 eV in the InP QD represented in Fig. 3(a), which compares with the value of 0.70 eV in the NW with similar diameter]. The interstitial position corresponding to the DX configuration becomes energetically more stable in the QDs than in the NWs.

The formation of DX centers is less favorable in the Se_P-doped InP NWs when compared to the NWs doped at the cation, as shown in the upper panel of Fig. 4 (circles and dotted line). The atomic displacements in the NWs only give metastable energy minimums for the smaller diameters, which quickly vanish as the diameter increases. These processes involve an In atom, which is initially bonded to the Se impurity. It is equivalent to the Si_{In}-doped NWs; the In atom breaks its bond with the impurity and displaces along axial or radial directions, finally assuming an interstitial position (see the middle panel of Fig. 4). The atom displaced is not the impurity

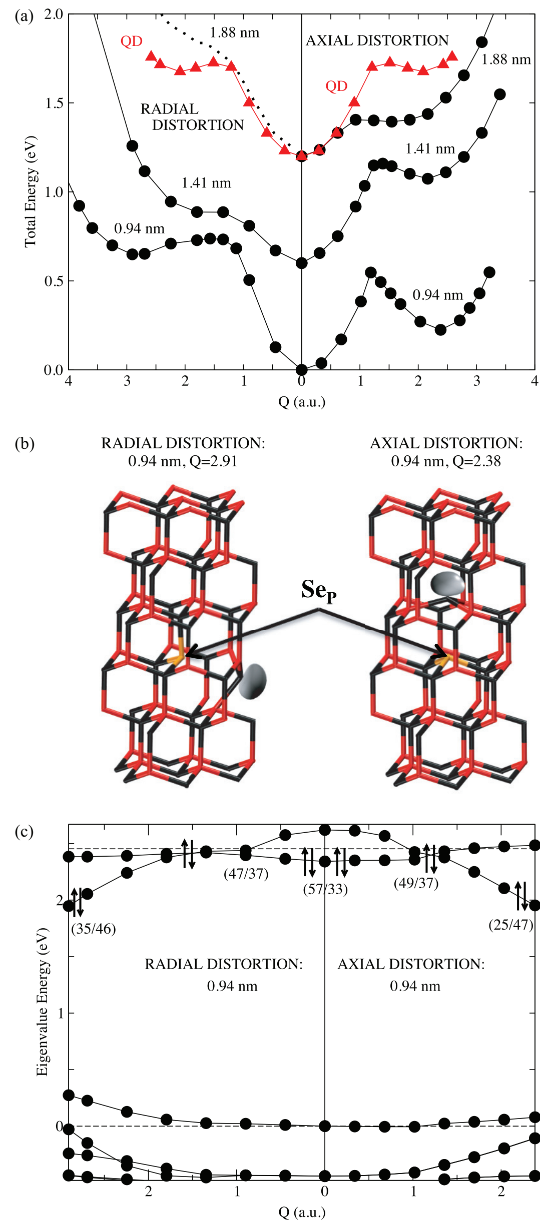

FIG. 4. (Color online) (a) Configuration coordinate diagrams of negatively charged Se_P-doped InP NWs obtained for axial and radial atomic displacements (circles). The dotted line for the NW with diameter 1.88 nm indicates that the energy curve was constructed from a single optimization process, and not from optimizations performed for fixed values of Q as in the rest of the curves. The configuration diagram of the negatively charged Se_P-doped InP QD with diameter 1.82 nm obtained in our previous work using the same theoretical approach is also shown (triangles; Ref. 5). (b) DX centers corresponding to the Se_P-doped InP NW with diameter 0.94 nm obtained by axial and radial atomic displacements. The charge density associated with the eigenstate holding the donor-electron pair is also shown. Black and red symbols stand for In and P atoms, respectively. Charge density is plotted at 40% of its maximum value. (c) Electronic structure of the negatively charged Se_P-doped InP NW with diameter 0.94 nm obtained for axial and radial atomic displacements. The arrows represent the impurity state holding the donor-electron pair, and the numbers in parentheses its projected s/p characters. Dashed lines correspond to CBM and VBM energy levels of the undoped NW that are used as a reference.

atom, but a first-neighbor atom. Again, this is consistent with electrostatic arguments. At $Q = 0$ the Se_P^- impurity is stable since it experiences Coulombic attraction from its four first neighbors, which are cation In atoms. The extra accumulation of electronic charge introduces some instability in its first neighbors, i.e., a Coulombic repulsion, since they are bonded to the ionized impurity and to three anion P atoms. Accordingly, the formation of the DX centers from the NW at $Q = 0$ implies overcoming higher energy barriers than in the Si_{In}-doped NWs (e.g., 0.55 and 0.74 eV for axial and radial displacements in the smallest NW, respectively, which compare with the values of 0.30 and 0.39 eV for the same NW doped by cation substitution).

The electronic structure of the Se_P-doped NWs show important differences (lower panel of Fig. 4). The energy lowering of the impurity state during the formation of the defect is less dramatic than in the Si_{In}-doped NWs [0.39 eV for the NW represented in Fig. 4(c)]; i.e., the impurity state becomes less deep and it contributes less to the stabilization of the DX centers. In the Se_P-doped NWs, the atom displaced is not the impurity, and there is no empty state located at the impurity that strongly interacts with the donor state, as discussed for the Si_{In}-doped NWs. The ionic dislocation just lowers an empty state with the same a_1 symmetry and CBM character as the impurity state. This state crosses the impurity level, finally capturing the electron-donor pair. Axial and radial displacements experience the same process. The high asymmetry showed by axial and radial total energy curves (upper panel of Fig. 4) should be attributed then to surface effects. Note that the displaced atom in the radial dimension is much closer to the surface than in the Si_{In}-doped NWs. Our results show that the formation of DX centers by radial atomic displacements is energetically more unfavorable in Se_P-doped NWs than in those NWs doped at the cation. In the upper panel of Fig. 4 we also include results from our previous study on n-type doped InP QDs;[5] i.e., we represent the configuration diagram for a Se_P-doped InP QD (triangles) with diameter similar to that of the biggest NW we studied. As explained, electrostatic and electronic structure aspects relevant to the formation of the defects are more accentuated in QDs than in NWs, and we again see how the formation of the defects is more favored in the former nanomaterials than in the latter. The configuration diagram for the nanocrystal shows a local energy minimum corresponding to the formation of the DX center, while in the NW with similar diameter such an energy minimum is absent.

As explained, the cause of stabilization of the DX centers is the electronic energy gain derived from the lowering of the position of the doubly occupied impurity state during the defect formation. The adequacy of the DFT-LDA in properly describing the stability of the DX centers follows by its capacity to describe this energy gain. In order to check this matter, we have performed calculations within the GW approximation,[21] starting from the electronic system in its DFT-LDA ground state as provided by the PARSEC code. We have computed quasiparticle GW energy levels of impurity states at both fourfold-coordinated and DX configurations that allow us to obtain the electronic energy gain. We did this for all the InP NWs with a diameter of 0.94 nm that we studied, i.e., InP NWs doped at both anion and cation sites with defects that occur along axial and radial directions. We found that DFT-LDA underestimates the electronic energy gain for all NWs by the same amount of 0.4 eV when compared to the GW results. This indicates that even DX centers become quantitatively more stable than predicted by DFT-LDA; the DFT-LDA approximation provides qualitatively good results.

Previous DFT-LDA work on bulk systems gave an increase on the stability of DX centers when an external pressure was intentionally applied to the systems.[22,23] This was done to partially correct the DFT-LDA band gap error. Our GW results are consistent with these previous results.

IV. SUMMARY AND CONCLUSIONS

In this work we examined formation energies and possible formation of DX defect centers in Si_{In}- and Se_P-doped InP NWs. We employed first-principles calculations based on a real-space pseudopotential approach, which is specifically targeted for applications at the nanoscale. We find the formation energies to increase monotonically with decreasing diameter of the NW as a result of the two-dimensional quantum confinement. The behavior of the formation energy is similar for both Si_{In} and Se_P dopants, showing quantitative differences in favor of the latter. In contrast, the results obtained for defect formation significantly differ. We find the formation of DX centers to be favored when the dopant is placed at the cation. Also, at this site, the defect formation implies electronic structure processes that put the donor impurity state deep within the band gap. We examined the DX formation as a function of quantum confinement. The anisotropic nature of the NWs discriminates between the formation of defects along axial and radial directions. We find defects that occur along the growth direction of the NWs to be preferential. Overall, our results show that the NWs should be n-type doped at the anion and not at the cation if they are to be used in functional devices within the deep nanometer regime. The comparison with our previous work on InP QDs also allows us to determine how a reduction in the dimensionality of semiconductor materials is against their n-type doping efficiency. We find that the formation energies of the dopants are bigger in QDs than in NWs for nanomaterials within the same diameter range, as well as their possibility in forming DX-like defect centers.

ACKNOWLEDGMENTS

This work was supported by the Spanish Ministry of Science and Innovation in conjunction with the European Regional Development Fund (Project No. FIS2012-33126). J.R.C. would like to acknowledge partial support from the Department of Energy for work on nanostructures from Grant No. DE-FG02-06ER46286. We also wish to acknowledge support provided by the Scientific Discovery through Advanced Computing (SciDAC) program funded by the US Department of Energy, Office of Science, Advanced Scientific Computing Research and Basic Energy Sciences, under Award No. DESC0008877 on algorithms. Computational support was provided in part by CESGA.

[*]manuel.alemany@usc.es

[1]C. M. Lieber and Z. L. Wang, MRS Bull. **32**, 99 (2007).
[2]G. Cantele, E. Degoli, E. Luppi, R. Magri, D. Ninno, G. Iadonisi, and S. Ossicini, Phys. Rev. B **72**, 113303 (2005).
[3]J. Han, T.-L. Chan, and J. R. Chelikowsky, Phys. Rev. B **82**, 153413 (2010).
[4]J. Li, S.-H. Wei, and L.-W. Wang, Phys. Rev. Lett. **94**, 185501 (2005).
[5]L. V. Besteiro, L. Tortajada, M. L. Tiago, L. J. Gallego, J. R. Chelikowsky, and M. M. G. Alemany, Phys. Rev. B **81**, 121307 (2010).
[6]C.-Y. Moon, W.-J. Lee, and K. J. Chang, Nano Lett. **8**, 3086 (2008).
[7]X. F. Duan, Y. Huang, Y. Cui, J. Wang, and C. M. Lieber, Nature (London) **409**, 66 (2001).
[8]Y. Huang and C. M. Lieber, Pure Appl. Chem. **76**, 2051 (2004).
[9]See http://parsec.ices.utexas.edu.
[10]J. R. Chelikowsky, M. M. G. Alemany, T.-L. Chan, and G. M. Dalpian, Rep. Prog. Phys. **74**, 046501 (2011); L. Kronik, A. Makmal, M. L. Tiago, M. M. G. Alemany, M. Jain, X. Y. Huang, Y. Saad, and J. R. Chelikowsky, Phys. Stat. Solidi (b) **243**, 1063 (2006); J. R. Chelikowsky, J. Phys. D **33**, R33 (2000).
[11]N. Troullier and J. L. Martins, Phys. Rev. B. **43**, 1993 (1991).
[12]D. M. Ceperley and B. J. Alder, Phys. Rev. Lett. **45**, 566 (1980).
[13]M. M. G. Alemany, X. Huang, M. L. Tiago, L. J. Gallego, and J. R. Chelikowsky, Solid State Commun. **146**, 245 (2008).
[14]M. M. G. Alemany, X. Huang, M. L. Tiago, L. J. Gallego, and J. R. Chelikowsky, Nano Lett. **7**, 1878 (2007).
[15]M. M. G. Alemany, L. Tortajada, X. Huang, M. L. Tiago, L. J. Gallego, and J. R. Chelikowsky, Phys. Rev. B **78**, 233101 (2008).
[16]X. Huang, E. Lindgren, and J. R. Chelikowsky, Phys. Rev. B **71**, 165328 (2005).
[17]M. S. Gudiksen, J. Wang, and C. M. Lieber, J. Phys. Chem. B **105**, 4062 (2001).
[18]D. J. Chadi and K. J. Chang, Phys. Rev. Lett. **61**, 873 (1988).
[19]D. J. Chadi and K. J. Chang, Phys. Rev. B **39**, 10063 (1989).
[20]This definition of formation energy is equivalent to the original definition of Chadi and Chang (Refs. 18 and 19) for substitutional donors with $U = 0$, as explained in Refs. 4 and 23–25.
[21]M. L. Tiago and J. R. Chelikowsky, Phys. Rev. B **73**, 205334 (2006).
[22]J. Ma and S.-H. Wei, Phys. Rev. B **87**, 115210 (2013).
[23]S.-H. Wei and S. B. Zhang, Phys. Rev. B **66**, 155211 (2002).
[24]M.-H. Du and S. B. Zhang, Phys. Rev. B **72**, 075210 (2005).
[25]M.-H. Du, Appl. Phys. Lett. **92**, 181908 (2008).